PROCEEDINGS OF SCIENCE

Strangeness S=-2 baryon-bayon interactions from lattice QCD

K. Sasaki*
Center of Computational Sciences, University of Tsukuba
Tsukuba, Ibaraki 305-8577, Japan
E-mail: `kenjis@het.ph.tsukuba.ac.jp`

for HAL QCD collaboration

We investigate baryon-baryon interactions with the strangeness $S = -2$ system in $2+1$ flavor lattice QCD, using gauge configurations provided by the CP-PACS/JLQCD Collaborations. The potential matrix is extracted by the Nambu-Bethe-Salpeter amplitudes from lattice QCD simulation through the $\Lambda\Lambda$, $N\Xi$, $\Sigma\Sigma$ and $\Lambda\Sigma$ coupled-channel Schrödinger equation. We confirmed that qualitative features of the potential matrix are consistent with those from SU(3) symmetric calculations and effects of SU(3) breaking in baryon-baryon interactions are still small even in the situation of $m_\pi \simeq 661$MeV and $m_\pi/m_K = 0.86$.

The XXIX International Symposium on Lattice Field Theory - Lattice 2011
July 10-16, 2011
Squaw Valley, Lake Tahoe, California

*Speaker.

PoS(Lattice 2011)173

1. Introduction

In recent years strangeness $S=-2$ multi-baryon systems attract much attention both theoretically and experimentally, since they are the first step toward the understanding of the multi-strangeness nuclear physics. At J-PARC experimental efforts in this field have been devoted to investigate structures of double-Λ hypernucleus, which is a nucleus with two-Λ's, and to search a Ξ hypernucleus. These investigations are expected to indirectly provide some informations of strangeness $S=-2$ baryon-baryon interaction. However, baryon-baryon scattering experiments with strangeness $S=-2$ are still thought to be very hard.

On theoretical side, it is important to complete the knowledge of the generalized nuclear force, which includes not only the nucleon-nucleon (NN) interaction but also hyperon-nucleon (YN) and hyperon-hyperon (YY) interactions, for the deeper understanding of atomic nuclei, structure of neutron stars and supernova explosions. A satisfactory theoretical description of the generalized nuclear force in phenomenological model approaches, however, had not existed yet due to the lack of the YN and YY scattering data in free-space, which is crucial to fix some model parameters such as a cutoff of interaction vertices and a size of hard cores. This situation starts changing by a series of investigations by HAL QCD collaboration [1, 2, 3, 4, 5, 6, 7], which determines baryon-baryon (BB) potentials in lattice QCD. Since potentials obtained in their method are faithful to the scattering phase shifts, the method would potentially be a complement to baryon-baryon scattering experiments.

As a related issue, it is interesting to investigate a possibility for an existence of a bound state in two-baryon system with $S=-2$. In the flavor $SU(3)$ symmetric world realized in lattice QCD, the investigation by the above method indicates an existence of the bound state in flavor singlet channel with strangeness $S=-2$ [8], which corresponds to the H-dibaryon state, first predicted by R. L. Jaffe in 1977 [9]. Even if the small $SU(3)$ breaking effect is introduced, by applying the conventional Lüscher formula, it is shown that the H-dibaryon state exists with the binding energy of ~ 17 MeV at $m_\pi \sim 389$MeV[10].

An aim of this work is to extend the potential description in the HAL QCD method to the case that the coupled channel analysis is necessary, in order to investigate BB interactions and the fate of the H-dibaryon at the physical quark masses with the (large) SU(3) breaking.

2. Potential matrix

A general form of the Schrödinger equation for the full wave function $\Psi(\vec{r},E)$ with a relativistic energy E is given as

$$\left[\tilde{E}-H_0\right]\Psi(\vec{r},E)=\int d^3\vec{r}'\,U(\vec{r},\vec{r}')\,\Psi(\vec{r}',E) \tag{2.1}$$

where H_0 is the free Hamiltonian, $U(\vec{r},\vec{r}')$ is an energy independent non-local potential and $\tilde{E}$ a non-relativistic energy obtained from the relativistic energy as $E-m_1-m_2\simeq\tilde{E}$. At low energies, the non-local potential can be expanded in terms of the velocity $\vec{v}=-i\vec{\nabla}/\mu$ as $U(\vec{r},\vec{r}')=(V_{LO}+V_{NLO}+V_{NNLO}+\cdots)\delta(\vec{r}-\vec{r}')$, where N^nLO term is of $O(v^n)$.

If we assume that the full wave function $\Psi(\vec{r},E)$ contains two independent states, denoted as α and β, eq. (2.1) leads to the following coupled channel Schrödinger equation at the leading order of the velocity expansion for the non-local potential.

$$\begin{aligned}\left(H_{0\alpha}+\tilde{E}_{\alpha}\right)\psi^{\alpha}(\vec{r},E) &= \sum_{\gamma=\alpha,\beta} V^{\alpha}{}_{\gamma}(\vec{r})\psi^{\gamma}(\vec{r},E)\\ \left(H_{0\beta}+\tilde{E}_{\beta}\right)\psi^{\beta}(\vec{r},E) &= \sum_{\gamma=\alpha,\beta} V^{\beta}{}_{\gamma}(\vec{r})\psi^{\gamma}(\vec{r},E)\end{aligned} \tag{2.2}$$

where free Hamiltonians and non-relativistic energies for channel α and β are given by

$$H_{0\alpha} = -\frac{\nabla^2}{2\mu_\alpha},\ \ H_{0\beta} = -\frac{\nabla^2}{2\mu_\beta},\ \ \tilde{E}_\alpha = E - m_{\alpha_1} - m_{\alpha_2} \simeq \frac{p^2}{2\mu_\alpha}\ \text{ and }\ \tilde{E}_\beta \simeq \frac{q^2}{2\mu_\beta} \tag{2.3}$$

with reduced mass μ and asymptotic momenta p and q related to energy of state as

$$E = \sqrt{m_{\alpha_1}^2+p^2}+\sqrt{m_{\alpha_2}^2+p^2} = \sqrt{m_{\beta_1}^2+q^2}+\sqrt{m_{\beta_2}^2+q^2}. \tag{2.4}$$

Therefore the potential matrix can be obtained from the equal-time Nambu-Bethe-Salpeter (NBS) wave functions through the coupled channel Schrödinger equation (2.2). This is an extension of the HAL QCD method[11].

The NBS wave function is defined with a local composite operator for a baryon $B(\vec{x})$ as

$$\psi^{B_1B_2}(\vec{r},E) = \sum_{\vec{x}}\langle 0 \mid B_1(\vec{x}+\vec{r})B_2(\vec{x}) \mid E\rangle, \tag{2.5}$$

which is extracted from the 4-point correlation function given by

$$W_{\mathscr{I}}^{B_1B_2}(t-t_0,\vec{r}) = \sum_{\vec{x}}\langle 0 \mid B_1(t,\vec{x}+\vec{r})\,B_2(t,\vec{x})\,\overline{\mathscr{I}}(t_0) \mid 0\rangle \ \propto A_E\,\psi^{B_1B_2}(\vec{r},E)e^{-E(t-t_0)} \tag{2.6}$$

for a moderate value of t, where $A_E = \langle E \mid \overline{\mathscr{I}}(t_0) \mid 0\rangle$ and $\mathscr{I}$ is a well-optimized source operator, which creates the eigenstate of the energy E with a baryon number $B=2$.

In order to extract BB potentials in the above method, we have to determine the asymptotic momenta p and q. For this purpose, we introduce a so-called R-correlator, defined by

$$R_{\mathscr{I}}^{B_1B_2}(t-t_0,\vec{r}) = e^{(m_1+m_2)(t-t_0)}W_{\mathscr{I}}^{B_1B_2}(t-t_0,\vec{r}) \propto A_E\,\psi^{B_1B_2}(\vec{r},E)e^{-(E-m_1-m_2)(t-t_0)} \tag{2.7}$$

where p is related to E by eq. (2.4). Using the non-relativistic expansion that $E-m_1-m_2 \simeq p^2/2\mu$, we can easily obtain the kinetic energy term by the time derivative of the R-correlator as

$$-\frac{\partial}{\partial t}R_{\mathscr{I}}^{B_1B_2}(t-t_0,\vec{r}) \propto \frac{p^2}{2\mu}A_E\,\psi^{B_1B_2}(\vec{r},E)e^{-(E-m_1-m_2)(t-t_0)}. \tag{2.8}$$

Combining a time dependent version of eq. (2.2) at two different $\mathscr{I}$'s (energies), we obtain

$$\begin{pmatrix} V^{\alpha}{}_{\alpha}(\vec{r}) \\ V^{\alpha}{}_{\beta}(\vec{r}) \end{pmatrix} = \begin{pmatrix} W^{\alpha}_{\mathscr{I}_1}(t,\vec{r}) & W^{\beta}_{\mathscr{I}_1}(t,\vec{r}) \\ W^{\alpha}_{\mathscr{I}_2}(t,\vec{r}) & W^{\beta}_{\mathscr{I}_2}(t,\vec{r}) \end{pmatrix}^{-1} \begin{pmatrix} -\frac{\nabla^2}{2\mu_\alpha}W^{\alpha}_{\mathscr{I}_1}(t,\vec{r}) - e^{(m_1+m_2)t}\frac{\partial}{\partial t}R^{\alpha}_{\mathscr{I}_1}(t,\vec{r}) \\ -\frac{\nabla^2}{2\mu_\alpha}W^{\alpha}_{\mathscr{I}_2}(t,\vec{r}) - e^{(m_1+m_2)t}\frac{\partial}{\partial t}R^{\alpha}_{\mathscr{I}_2}(t,\vec{r}) \end{pmatrix}. \tag{2.9}$$

This extraction of the potential matrix is valid as long as $\mathscr{I}_1$ and $\mathscr{I}_2$ generate linearly independent wave functions. Suppose that optimized source operators, $\mathscr{I}_1$ and $\mathscr{I}_2$, are constructed from two-baryon operators $\mathscr{I}_A$ and $\mathscr{I}_B$ as

$$\begin{pmatrix} \mathscr{I}_1 \\ \mathscr{I}_2 \end{pmatrix} = \begin{pmatrix} U_1{}^A & U_1{}^B \\ U_2{}^A & U_2{}^B \end{pmatrix}\begin{pmatrix} \mathscr{I}_A \\ \mathscr{I}_B \end{pmatrix}, \tag{2.10}$$

eq.(2.9) is valid also for a pair $\mathscr{I}_A$, $\mathscr{I}_B$, as long as the matrix U is invertible. Therefore optimized source operators are NOT necessary to extract the potential matrix. This property is an advantage of the time-dependent Schrödinger type equation over the equation (2.2).

Table 1: A number of gauge configurations and calculated hadron masses in unit of [MeV].

N_{conf}	m_π	m_K	m_N	m_Λ	m_Σ	m_Ξ
800	661(1)	768(1)	1482(3)	1557(3)	1576(3)	1640(3)

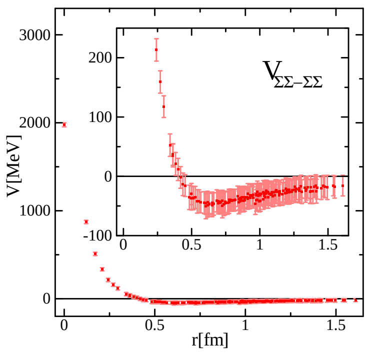

Figure 1: Potential in the $^1S_0(I=2)$ channel

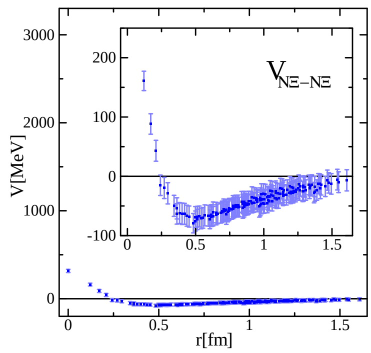

Figure 2: Potential in the $^3S_1(I=0)$ channel

3. Numerical simulations

In the calculation we employ $2+1$-flavor full QCD gauge configurations from Japan Lattice Data Grid(JLDG)/International Lattice Data Grid(ILDG) [13]. They are generated by the CP-PACS and JLQCD Collaborations with a renormalization-group improved gauge action and a non-perturbatively $O(a)$ improved clover quark action at $\beta = 6/g^2 = 1.83$, corresponding to lattice spacings of $a = 0.1209$ fm [14], on $L^3 \times T = 16^3 \times 32$ lattice, about $(2.0 \text{ fm})^3 \times 4.0$ fm in physical unit. The hopping parameter are given by $\kappa_{u,d} = 0.13825$ for light quarks and $\kappa_s = 0.13710$ for the s-quark. Quark propagators are calculated with the spatial wall source at t_0 with the Dirichlet boundary condition in temporal direction at $t = 16+t_0$. An average over the cubic group is taken for the sink operator, in order to obtain the S-wave in the BB wave function. Numerical computation have been carried out on the kaon and jpsi clusters at Fermilab. Calculated hadron masses are given in Table 1.

4. Results

The potential matrices V^i_js calculated by using the NBS wave functions at $t-t_0 = 9$ are shown in Figures 1-5. A symmetric difference in t is employed for the time derivative term in this paper.

We first consider the single channels, $^1S_0$ with $I=2$ and $^3S_1$ with $I=0$. Fig. 1 shows the potential in the $^1S_0$ and $I=2$ channel. This potential corresponds to the 27-plet in the SU(3) irreducible representation, to which the NN potential belongs. As in the case of the NN potential, we observe a repulsion at short short distance while an attraction at long distance. The potential in the $^3S_1$ and $I=0$ channel, which has an one-to-one correspondence with the 8_a-plet, is shown in Fig. 2. A repulsion at short distance is expected to be weak since the Pauli blocking effect is not strong in this channel according to the constituent quark model. Our result in Fig. 2 is consistent with this expectation.

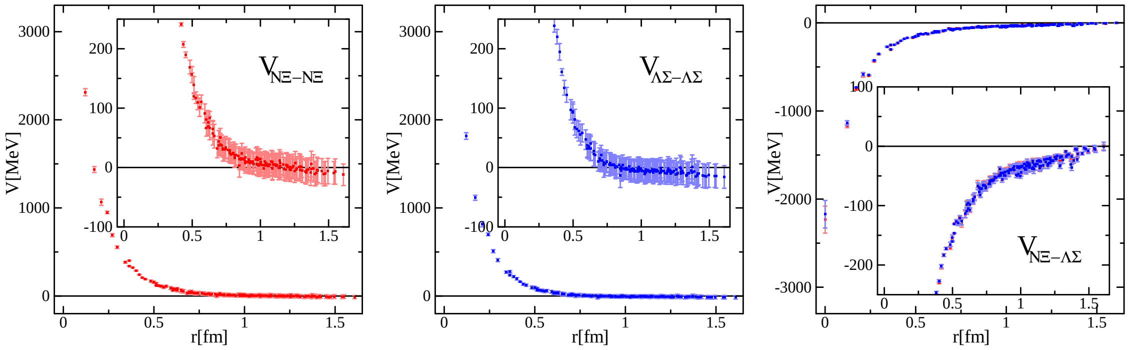

Figure 3: Elements of potential matrix in the $^1S_0(I=1)$ channel

.

The potentials in the $^1S_0$ and $I=1$ channel, obtained by solving 2×2 coupled channel equations, are shown in Fig. 3. As seen in the SU(3) symmetric calculation[4], diagonal elements of the potential matrix in this channel, $V_{N\Xi-N\Xi}$ and $V_{\Lambda\Sigma-\Lambda\Sigma}$, are both strongly repulsive and transition potentials between $N\Xi$ and $\Lambda\Sigma$ states become large at the short distance.

Potential matrices in the $^3S_1$ with $I=1$ and $^1S_0$ with $I=0$ channels are shown in Figs. 4 and 5, respectively. In both cases, the potential matrix is calculated from 3×3 coupled channel equations.

In Fig. 4, all diagonal potentials have a mid-range attraction and a repulsion at short distance (repulsive core) which are not so strong comparing to the other channels. The largest attraction in this channel is seen in the diagonal $\Sigma\Sigma$ potential. Transition potentials between $\Lambda\Sigma$ channel and $N\Xi$ or $\Sigma\Sigma$ channel are much smaller than the $N\Xi$ - $\Sigma\Sigma$ transition potential. A smallness of the former transition potentials indicates that the $\Lambda\Sigma$ channel is more or less isolated from other channels.

Finally, we consider the potential matrix in the $^1S_0$ and $I=0$ channel, in which the H dibaryon state appears if exists. As shown in Fig. 5, all diagonal components of the potential matrix have a repulsion at short distance. The strength of the repulsion in each channel, however, varies, reflecting properties of its main component in the irreducible representation of the flavor SU(3): The diagonal potential in the $\Sigma\Sigma$ channel, whose main component is the symmetric-octet in SU(3), is most repulsive, since the symmetric-octet has the strongest repulsion at all distances in the SU(3) limit[4] and this property holds even with the SU(3) breaking. On the other hand, diagonal potentials in $N\Xi$ and $\Lambda\Lambda$ channels has not only a repulsion at short distance but also an attraction at medium distance, due to a mixture between the repulsive symmetric-octet potential and the attractive flavor singlet potential[4]. It is noted that the $\Lambda\Lambda$ - $N\Xi$ transition potential is smaller than other transition potentials. Therefore, the $N\Xi$ to $\Lambda\Lambda$ decay rate is expected to be relatively suppressed. This property favors a formation and an observation of the Ξ hypernuclei in experiments.

5. Conclusions

We have investigated the $S=-2$ BB potentials from $2+1$ flavor lattice QCD by considering the $\Lambda\Lambda$, $N\Xi$, $\Sigma\Sigma$ and $\Lambda\Sigma$ coupled channels. By using the extended HAL QCD method for coupled channels [11, 12], we successfully extract a potential matrix for a coupled channel. Combining the

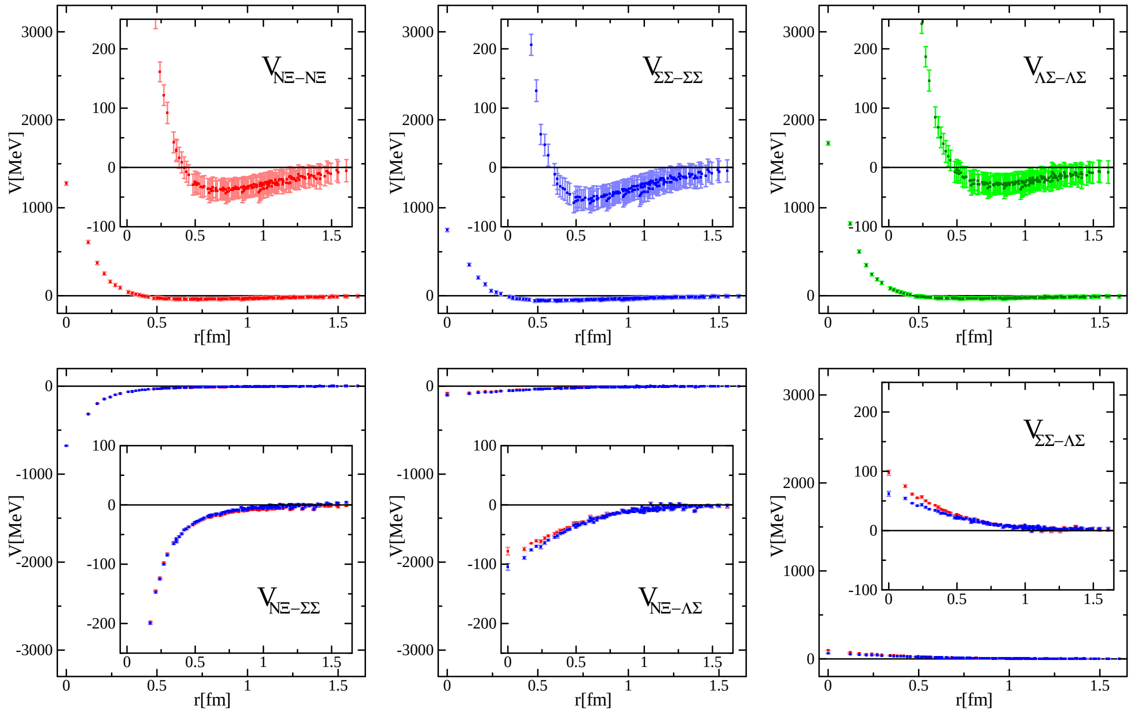

Figure 4: Elements of the potential matrix in the ${}^3S_1(I=1)$ channel

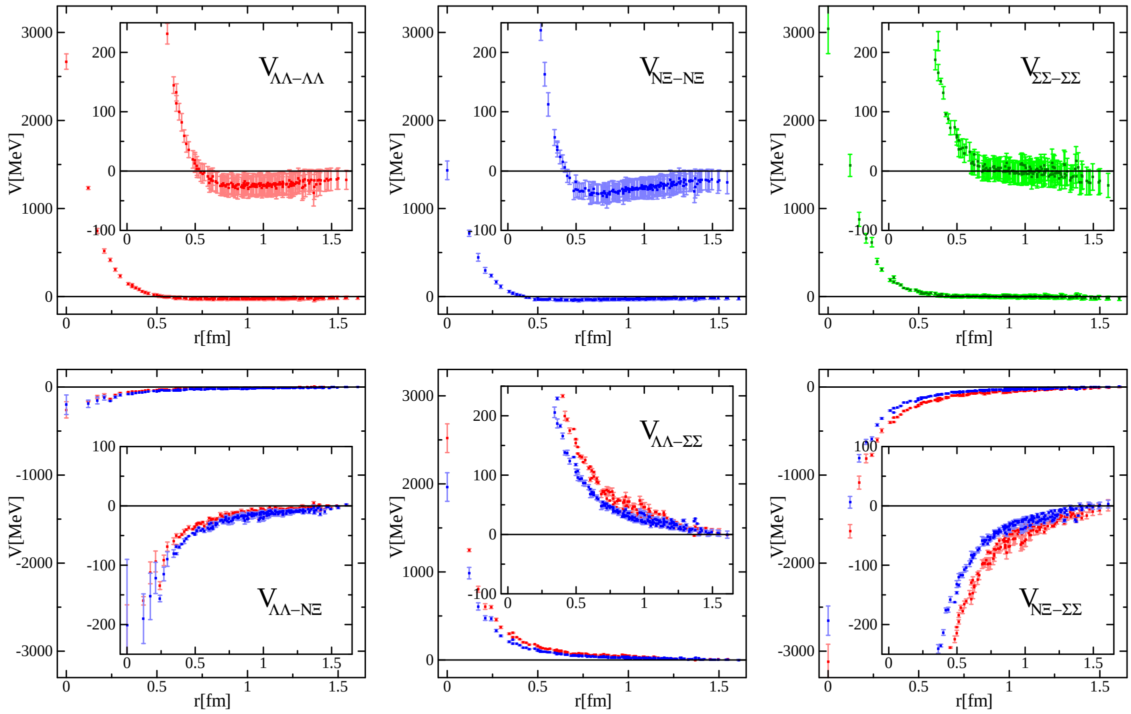

Figure 5: Elements of the potential matrix in the ${}^1S_0(I=0)$ channel

coupled channel formalism with the time-dependent Schrödinger type equation [12], we can get rid of ambiguities of potential and avoid the diagonalization procedure for the source operators.

We have found that potentials in particle basis with the SU(3) breaking have similar properties to those of unitary rotated *BB* potentials in SU(3) limit [4]. In this calculation, however, effects of SU(3) breaking are still small, so we will introduce larger SU(3) breaking effects in future investigations.

Acknowledgement

We greatly appreciate members of the USQCD Executive Committee for their offer of computer resources to overcome the electricity crisis due to the Catastrophic Earthquake in East of Japan on Mar. 11th. We are grateful for authors and maintainers of CPS++ [15], whose modified version is used for our simulations. We also thank CP-PACS Collaboration and ILDG/JLDG [13] for providing gauge configurations. This work is supported in part by SPIRE(Strategic Programs for Innovative REsearch) , Grant-in-Aid of the Ministry of Education, Science and Technology, Sports and Culture (Nos. 20340047, 22540268, 19540261) and the Grant-in-Aid for Scientific Research on Innovative Areas (No. 2004:20105001,20105003).

References

[1] N. Ishii, S. Aoki and T. Hatsuda, Phys. Rev. Lett. **99** (2007) 022001.

[2] S. Aoki, T. Hatsuda and N. Ishii, Prog. Theor. Phys. **123** (2010) 89.

[3] H. Nemura, N. Ishii, S. Aoki and T. Hatsuda, Phys. Lett. B**673** (2009) 136.

[4] T. Inoue *et al.* [HAL QCD collaboration], Prog. Theor. Phys. **124** (2010) 591

[5] Y. Ikeda *et al.*, arXiv:1002.2309 [hep-lat].

[6] K. Murano, N. Ishii, S. Aoki and T. Hatsuda, Prog. Theor. Phys. **125** (2011) 1225

[7] T. Doi *et al.*, arXiv:1106.2276 [hep-lat].

[8] T. Inoue *et al.* [HAL QCD Collaboration], Phys. Rev. Lett. **106** (2011) 162002

[9] R. L. Jaffe, Phys. Rev. Lett. **38** (1977) 195 [Erratum-ibid. **38** (1977) 617].

[10] S. R. Beane *et al.* [NPLQCD Collaboration], Phys. Rev. Lett. **106** (2011) 162001

[11] S. Aoki *et al.* [HAL QCD Collaboration], Proc. Jpn. Acad., Ser. B, **87** (2011) 509.

[12] N. Ishii for HAL QCD collaboration, in these proceedings.

[13] See "http://www.lqcd.org/ildg" / "http://www.jldg.org"

[14] T. Ishikawa *et al.* [CP-PACS/JLQCD Collaboration], Phys. Rev. D **78** (2008) 011502(R).

[15] Columbia Physics System(CPS), http://qcdoc.phys.columbia.edu/cps.html